J. Applied Membrane Science & Technology, Vol. 29, No. 1, April 2025, 55-72

Refined Assessment of the Impact of Membrane Module Channel Curvature on Pressure Drop

S. V. Huliienko*, V. V. Yasenchuk & M. O. Protsiuk

Faculty of Chemical Engineering, National Technical University of Ukraine "Igor Sikorsky Kyiv Polytechnic Institute", 37 Beresteiskyi Ave., 03056 Kyiv, Ukraine

Submitted: 11/11/2024. Revised edition: 16/1/2025. Accepted: 16/1/2025. Available online: 27/3/2025

ABSTRACT

Spacers are key components of membrane modules that significantly influence the performance of membrane separation processes and the value of pressure drop. The development of computational fluid dynamics (CFD) methods promoted a significant increase in investigation dedicated to improving spacer designs. However, some issues in this field remain controversial. One of them is the reasonability of the application of flat models during analysis processes in spiral-wound modules. In the current work, the CFD investigation of the influence of channel curvature on pressure drop was carried out using the open-source software package OpenFOAM-v2212. It was found that within the range of radii of curvature from 0.01 m (10 mm) to 0.025 m (25 mm) and lengths from 0.008 m (8 mm) to 0.015 m (15 mm), the discrepancy does not exceed 10%. Thus, the flat model can be considered an acceptable approximation of real conditions in spiral-wound module channels, particularly during the investigation of new spacer designs. However, if the observed effect does not exceed 7–10%, investigations that consider the channel curvature are advisable. The assumption about the existence of a critical value for the channel's radius of curvature was not confirmed. The influence of the mesh dimensions on the accuracy of simulation results was evaluated.

Keywords: Hydrodynamics, simulation, CFD, pressure drop, curvature

1.0 INTRODUCTION

Spacers are key components of membrane modules that facilitate feed flow through the membrane module. Additionally, the configuration of spacers in the channel has a significant influence on the hydrodynamic and mass transfer conditions of the process [1], as well as fouling [2] and thermal effects in non-isothermal processes such as membrane distillation [3]. Moreover, Hu *et al*. [1] note that the influence of spacers is particularly important for spiral-wound modules, which have the widest practical application, as shown in the work [4].

Taking this into account, a significant number of studies have been carried out dedicated to the impact of spacers on virtually all existing commercial membrane processes. For instance, reverse osmosis was considered in works [5-6], works [7-8] are dedicated to nanofiltration, and works [9-10] are focused on ultrafiltration. In addition to pressure-driven membrane processes, membrane distillation [11-12], electrodialysis [13-14], and forward osmosis [15-16] were considered.

In the significant number of works considered above [1-3, 6-15], advanced spacer designs adapted to the specific requirements of the considered in these studies processes were proposed. It is also should be noted

* Corresponding to: S. V. Huliienko (email: sergiiguliienko@gmail.com)
DOI: https://doi.org/10.11113/jamst.v29n1.310

that, in most of these works, the efficiency of spacers was primarily analyzed using computational fluid dynamics (CFD) methods [1-3, 6-8, 10-14] the effectiveness of them has been demonstrated not only for membrane channels with spacers [3, 17-19].

However, despite the substantial number of studies on spacer efficiency in channels using CFD methods, there are still some discussion issues that were outlined in our previous work [20]. In particular, it was pointed out that in works [21] and [22], different results were obtained when comparing the actual geometry of spacers with the idealized geometry created for CFD analysis. Hostermeier *et al*. [22] concluded that ignoring the real geometry could lead to significant errors, whereas Haaksman *et al*. [21] considered the idealized cylindrical shape of spacer filaments to be an acceptable approximation.

In work [20], the main attention was dedicated to the issue of the influence of the channel curvature on pressure drop. In particular, it was noted that in several studies, such as [23-24], as well as [1-3, 6-8, 10-14], the flat model was applied, whereas the spiral-wound module is the most commonly used membrane module type in practice [1, 4], except the case of electrodialysis [13-14]. At the same time, Taherinejad *et al*. [25] demonstrated that channel curvature can significantly influence the operating parameters of membrane processes, and neglecting this curvature may result in significant errors.

In work [20], the investigation of the impact of channel curvature on pressure drop, which is one of the most important parameters of membrane module performance [26] was carried out. The study was carried out by comparing the pressure drop for the ring-shaped channel and the same channel rolled out into the plate. The results showed that the difference in pressure drop between these channels did not exceed 3.2%, and some regularities in the pressure drop change with changes in some geometrical parameters in particular the length-to-diameter ratio was pointed out were observed. However, the slight increase in the difference with the increase in the radius of curvature was unexpected.

Although the results of the previous study [20] suggest that the flat model is an acceptable approximation, these findings require further refinement. Especially, not enough attention was paid to the validation of the reproduction of the results for each channel by repeated calculations during analysis of the results. Moreover, in the methodology used for comparison in that study, increasing the radius of curvature led to an increase in the volume of the analyzed element, which could have influenced the accuracy of the results. Additionally, the values of the radius of curvature in that study were limited to the dimensions of the spiral-wound membrane module of 1812 type, whereas the radius at which the channel curvature might have a significant impact could be smaller than the radius of the central tube.

Therefore, the aim of this work is to refine the impact of channel curvature on the pressure drop of the channel. For this purpose, CFD analysis should be performed on computational elements with equivalent volumes. As in work [20], the simulations were carried out for hypothetical channels without spacers.

2.0 METHODS

2.1 Theoretical Background

In work [20], it was pointed out that the fluid flow is described by the Navier-Stokes equations, the continuity

equation, and, where necessary, the mass and energy conservation equations and turbulence models can be applied. In this study, as in the previous one [20], the analysis is limited to the consideration of the pressure drop, therefore, there is no necessity to use mass and energy conservation equations. Also, similarly to work [20], the values of fluid flow velocities corresponding to the experimental values reported in the study [27] were used in simulations. In this case, the values of the Reynolds number did not exceed 20. In the absence of turbulence-inducing elements in the channel, it is evident that the flow under these conditions remains laminar, and thus, a turbulence model is not applied.

Therefore, under the considered conditions, the Navier-Stokes equations supplemented by the continuity equations are sufficient to describe the fluid flow.

In a compact operator form, the Navier-Stokes equations can be expressed as follows [28]:

$$\rho(\bar{u}\cdot\nabla)\bar{u} + \nabla P - \mu\nabla^2\bar{u} = 0 \qquad (1)$$

where $\bar{u}$ is the velocity vector, m/s; P is the pressure vector, Pa ρ is the fluid density, kg/m^3; μ is the dynamic viscosity coefficient, Pa·s; ∇ the Hamiltonian operator; ∇^2 the Laplace operator.

The continuity equation in operator form can be written in following way [28]:

$$\nabla\cdot\bar{u} = 0 \qquad (2)$$

The full forms of these equations are provided in works [4, 20, 24].

The boundary conditions used in the simulations were also similar to those in study [20] and can be expressed as:

$$\begin{cases} \bar{u} = 0 \text{ at all walls} \\ u_y = u_{y0} \text{ at } y = 0 \\ P = P_{static} \text{ at } y = l \end{cases} \qquad (3)$$

where $\bar{u}$ is velocity vector, m/s, u_{y0} is initial value of uniform velocity, m/s, P_{statoc} is the value of the static pressure, Pa; l is the length of channel, m.

2.2 Software Used for Simulation

In work [4], it is shown that specialized software plays a key role in CFD simulation. It is also noted that alongside commercial software products such as ANSYS and COMSOL, open-source software like OpenFOAM can be used [4, 20]. The effectiveness of the latter for the simulation of membrane processes has been demonstrated in studies [29-36], as well as for simulating other processes in chemical engineering [37-40]. Accordingly, in this study, as in the previous work [20], the simulation was carried out using the OpenFOAM-v2212 software package. The choice of this version was made for the same reasons as in the study [20], specifically because it can be integrated into the FreeCAD CAD system. Similarly, for creating the geometry of the studied objects and post-processing the modeling results, the same software products were used as in [20], namely FreeCAD 0.21.1 and ParaView 5.10.1, respectively.

2.3 Geometric Considerations

As it was mentioned above, in work [20], the values of radii of the channel curvature were limited to the dimensions of the module of 1812 type. This choice was due to the fact that this is one of the smallest commercially available spiral wound modules. Therefore, the values of radii of the channel curvature in such modules will be maximal, thus, the

impact of curvature in this case also will be maximal.

The spiral wound membrane module (Figure 1) consists of the membrane package, which includes the membranes and drainage material for permeate, and feed spacerб that are wrapped around a perforated central tube. At that, the roll layers formed the channel for the feed solution passage. The permeate is removed through the central tube, and the retentate comes out of the opposite end [1, 2]

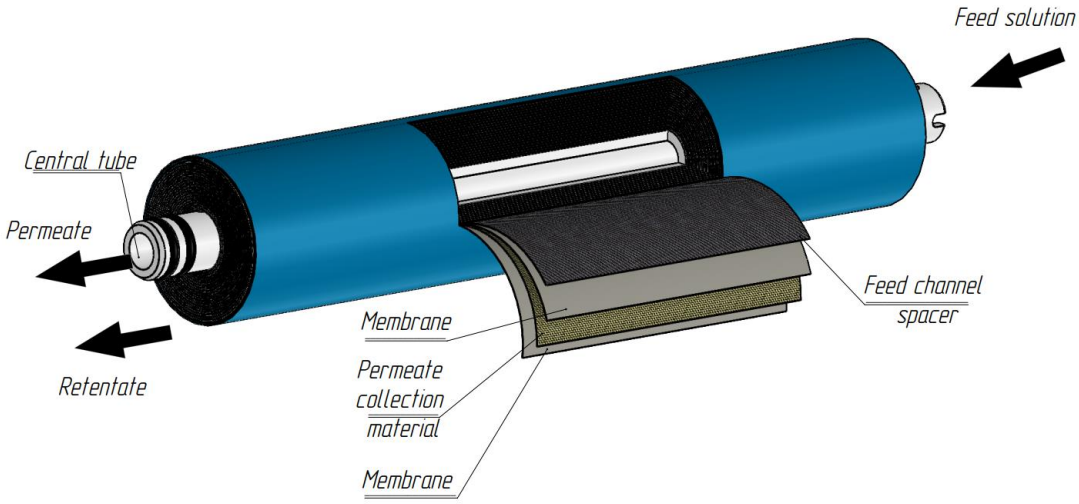

Figure 1 Schematic representation of the spiral module design

It can be seen from Figure 1, that the channels have a curved shape. Herewith, Taherinejad *et al.* [25] pointed out, that the channel curvature determines the nonuniformity in the shear stress field on the channel surfaces with different radii, which could lead to the forming of additional vortexes, turbulations, stagnant zones, etc. Consequently, the pressure drop can increase, in the zones of increased velocity, the mass transfer coefficient can increase, and in the stagnant zones, the opposite effect can be observed from the point of view of mass transfer. Also, these phenomena can facilitate fouling formation. Therefore, the study of the influence of the channel curvature is reasonable. Due to the overall complexity of the problem, in this work, the consideration is limited to the hydrodynamics issue.

As it was mentioned above, in work [20], the values of the pressure drop in ring-shaped channels were compared with corresponding values in flat channels, which were the ring-shaped rolled out onto the plane, with the aim of determining the effect of channel curvature on the pressure drop. The attempts to carry out detailed investigations with such channels led the controversial results. The probable reason for this was that in this case, an increase in the channel curvature radius led to an increase in the cross-sectional area of the channel and the volume of the element under investigation. Therefore, for a more accurate comparison, configurations with the same cross-sectional area but different curvature radii were chosen.

In the flat model, the cross-sectional area was represented by a rectangle with a height of 0.001 m (1 mm), which corresponded to the commonly used channel thickness with a spacer, in particular, the same value was used in work [3]. The width of the channel was chosen as 0.01 m, which is greater than the typical size between spacer filaments, which, according to the data

in work [2], is 0.0036 m (3.6 mm). In other cases, the radius of curvature of the centerline was varied from 0.0025 m (2.5 mm) to 0.025 m (25 mm) in steps of 0.0025 mm (2.5 mm). Figure 2 demonstrates the shape of the cross-section of each element (radius values are given in mm) and also the placement of the geometrical models selected for analysis by the cross-section of module 1812. It can be seen (Figure 2b) that most of the models correspond to placement within the dimension of the module, three models have a radius less than the central tube, and one module is bigger than the external diameter of the module. Additionally, part of the three-dimensional models of the channels under investigation are shown in Figure 3.

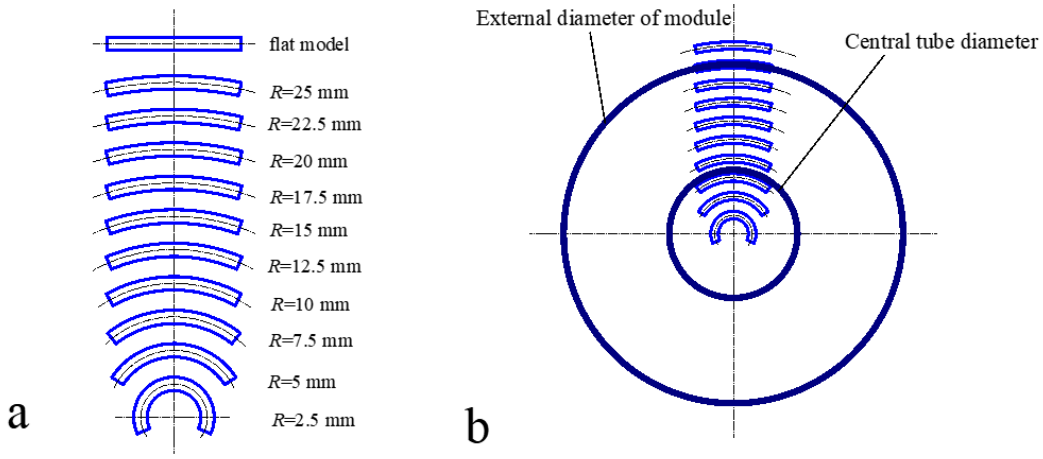

Figure 2 The shape of the cross-sections of the channels under investigation (a) and its location on the module cross-section (b)

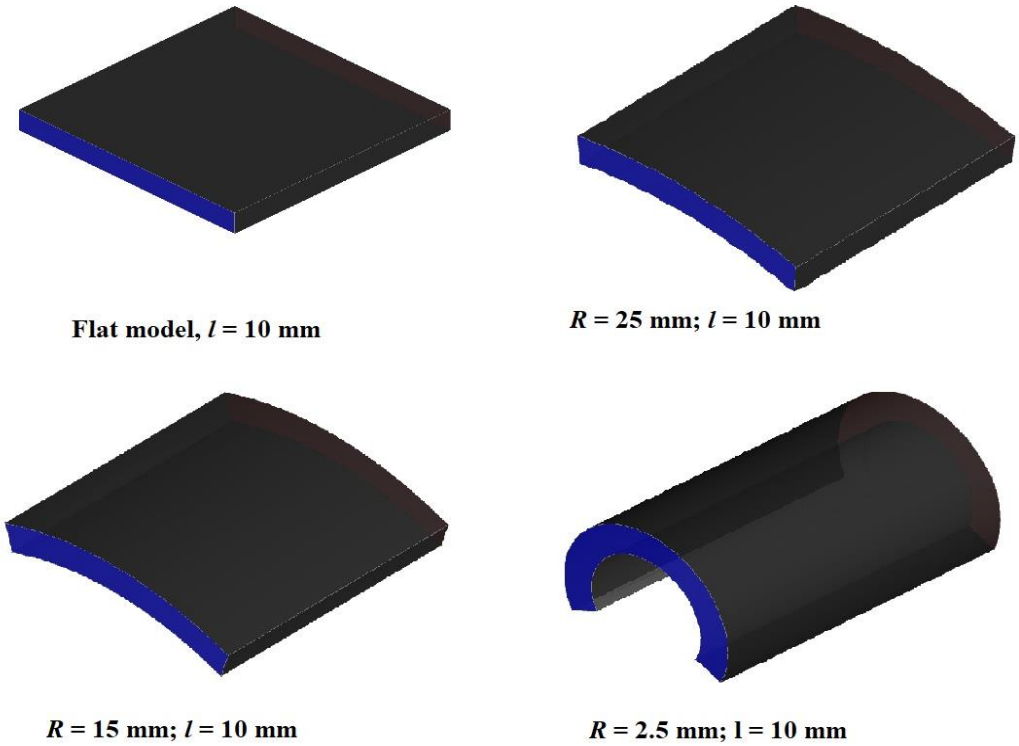

Figure 3 Three-dimensional models of some of the channels under investigation

2.4 Simulation Conditions

As in work [20], the conditions in the membrane modules of 1812 type were imitated during the CFD investigations. These conditions were defined in the experimental study in the previous work [27]. In particular, according to [27], the most rational conditions corresponded to an operating pressure of 0.5 MPa, at which the flow velocity was approximately 0.01 m/s. Accordingly, this value was used in the simulations. These velocity values corresponded to Reynolds numbers values less than 20, which, as mentioned in section 2.1, corresponds to a laminar flow regime thus, the laminar model was used in the simulations. Additionally, the properties of water (density and dynamic viscosity) were chosen as the fluid properties since the study in [27] was carried out with aqueous salt solutions. Since most membrane processes are isothermal, the liquid properties were considered as constants.

As a result, the accepted assumption can be listed in the following way:

-The flow in the channels is laminar

-The conditions are isothermal

-The physical properties of the medium are constant

-The geometry of channels is ideal

-The velocity on the walls is equal to zero

-The velocity on the entrance in the channel is uniform.

The boundary conditions, according to information presented above and in section 2.1, were the following. For the flat model, wall conditions (no-slip conditions) were set on the lower, upper, and side walls, indicated in black in Figure 2. Uniform velocity inlet conditions were applied at the front face (blue in Figure 2), and static pressure outlet conditions were set at the rear face. This fully matched the boundary condition selection in the work [20]. For all other channels, the boundary conditions were the same, except that the upper and lower surfaces were not flat but cylindrical, as shown in Figure 3.

In work [20], the mesh cell size in all elements was $0.1 \cdot 10^{-3}$ m (0.1 mm), which was not sufficiently substantiated. Therefore, the impact of cell size was also separately studied

3.0 RESULTS AND DISCUSSION

3.1 Profiles of velocity and pressure in the channels under investigation

The preliminary evaluation of the influence of the curvature of the channel on flow characteristics was realized by comparing the visualizations of velocity fields created in the ParaView 5.10.1 software. Figures from 4 to 6 represent part of these visualizations. In particulate, the velocity field in the cross-section in the middle of the channel lengths is shown in Figure 4.

Figure 5 demonstrates the velocity field in the longitudinal section, made along the middle plane of the flat channel and along the central radius of the curved channels. The pressure field is shown in Figure 6. In work [20], it was pointed out that in OpenFOAM, the results are presented in the form of kinematic pressure, i.e., the ratio of pressure to the density of the medium. Accordingly, the kinematic pressure values at various points in the channel are shown in Figure 5. The presented research results were obtained for a cell size of $0.05 \cdot 10^{-3}$ m (0.05 mm).

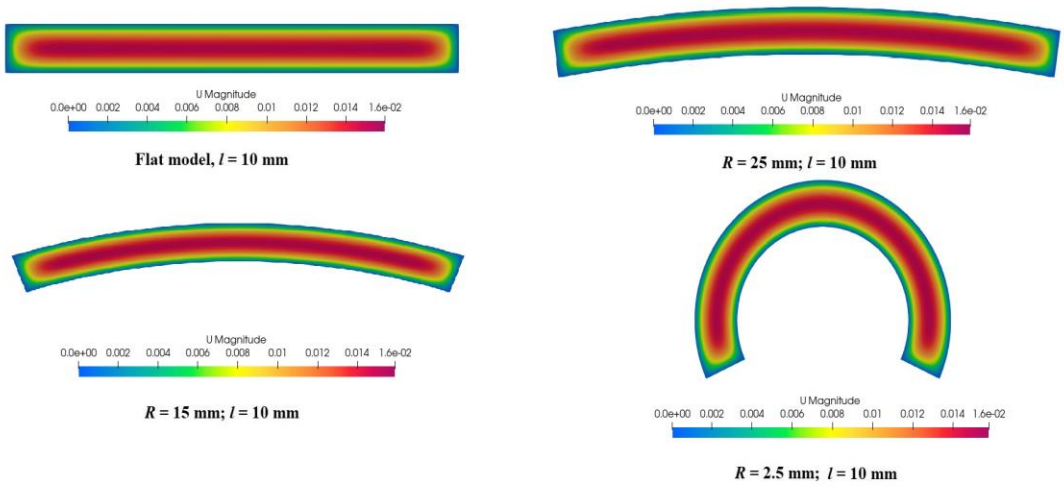

Figure 4 The velocity fields in the cross-sections of some of the channels under investigation

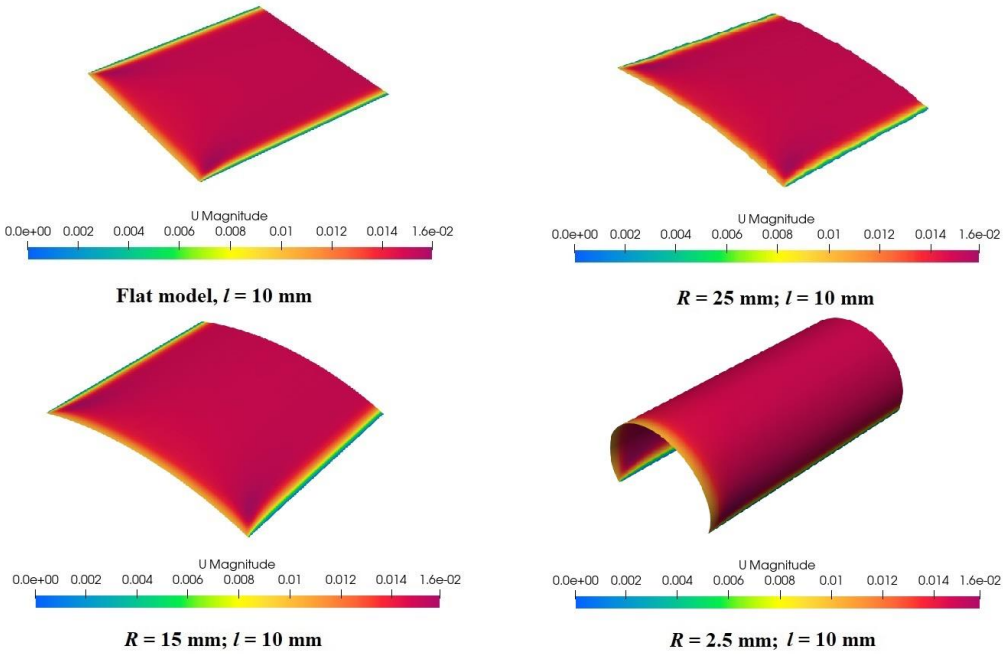

Figure 5 Velocity fields in the longitudinal cross-sections of some of the channels under investigation

No clear differences were observed between the velocity fields in the straight and curved channels, unlike in the study [22], where discrepancies between the real and ideal filament shapes of the spacer were clearly visible. Also, as in the case of the study [20], the velocity field generally corresponds to laminar flow conditions, with the maximum velocity at the center of the channel and a gradual decrease near the walls. It also should be noted that the velocity fields on the boundary surfaces appear similar, in contrast to some differences observed in [20], which suggests that the model chosen in the current study is more representative than in the previous one.

The kinematic pressure fields, shown in Figure 6, also correspond to the results and patterns of pressure drop in laminar flow, as described in [20].

The results, represented in Figures 4 to 6 are obtained for the channel shown in

Figure 2, which are typical. No differences were found for other channels.

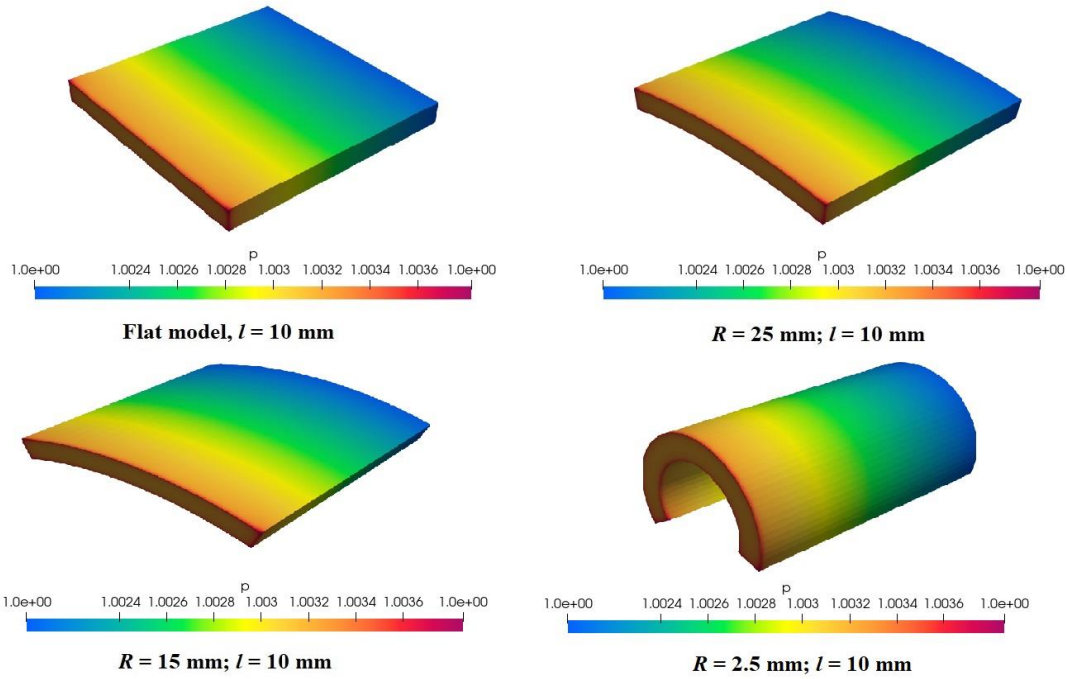

Figure 6 Kinematic pressure fields in some of the channels under investigation

3.2 Pressure drop in the channels under investigation

Although the visual assessment did not show significant differences in the flow pattern, it does not allow us to make definitive conclusions about the magnitude of the difference. Therefore, the set of simulations was carried out with different radii of curvature and channel lengths, as well as for a flat channel with the same length values. In all simulations, the mesh cell size was $0.05 \cdot 10^{-3}$ m (0.05 mm). The snippet of the results is shown in Figure 7.

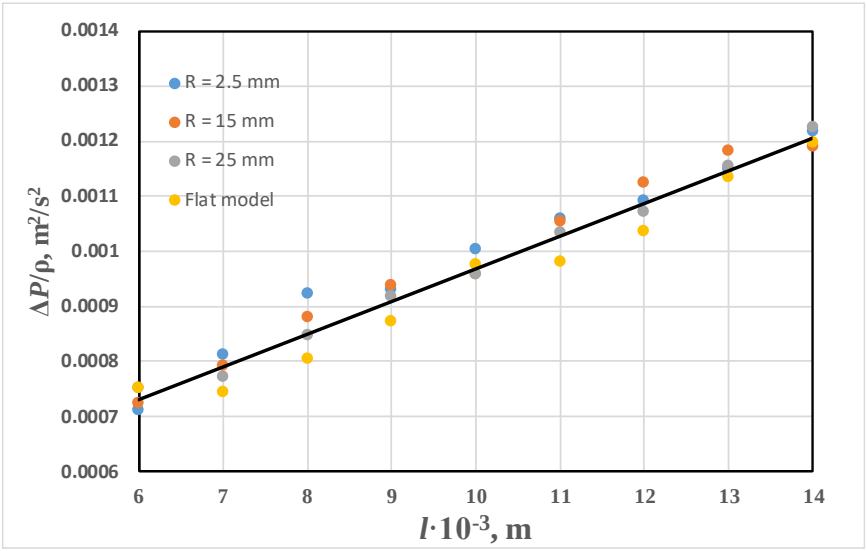

Figure 7 The pressure drop in the some channels versus the channel length

From this figure, it can be seen that the pressure drop values in the different channels are quite close. Although there is some scatter in the points, the results can be approximated by a straight line, which is in agreement with the commonly accepted understanding of pressure drop in channels under the considered flow conditions, as shown in the work [20]. However, due to the close pressure drop values for different radii of curvature, the visual distinction is not very high so the results will be presented in tabular form below.

The values of the pressure drop (kinematic pressure) from all the simulations are represented in Table 1 and Table 2 shows the difference in the pressure drop for channels with different radii of curvature compared to the flat model. The values of differences were calculated in the same way as in the work [41]:

$$e_p = \frac{\Delta P_{ri} - \Delta P_f}{\Delta P_{ri}} \cdot 100\% \qquad (4)$$

where ΔP_f is the pressure drop in a flat channel, m^2/s^2; ΔP_{ri} is pressure drop in a channel with the current radius of curvature, m^2/s^2.

Table 1 The pressure drop values in channels for different diameters, m^2/s^2

***R*, mm**	***l*, mm**				
	6	**7**	**8**	**9**	**10**
2.5	0.00071	0.00081	0.000922	0.00093	0.001002
5	0.000752	0.00083	0.000865	0.000933	0.000964
7.5	0.000701	0.000771	0.000875	0.000916	0.000946
10	0.000745	0.000796	0.000833	0.000957	0.00099
12.5	0.000708	0.000798	0.000869	0.000895	0.001018
15	0.000723	0.00079	0.000879	0.000936	0.000956
17.5	0.000732	0.000778	0.000865	0.000894	0.000983
20	0.000705	0.000774	0.000858	0.00089	0.000982
22.5	0.000835	0.000827	0.000835	0.000901	0.000947
25	0.00075	0.000771	0.000847	0.000918	0.000956
Flat model	0.000752	0.000743	0.000805	0.000873	0.000975
R, mm	*l,* mm				
	11	12	13	14	15
2.5	0.001057	0.00109	0.001149	0.001217	0.001298
5	0.001039	0.00107	0.001157	0.001267	0.001276
7.5	0.001007	0.001118	0.001164	0.001194	0.001309
10	0.001048	0.001082	0.00116	0.001213	0.00126
12.5	0.001064	0.001116	0.001146	0.001189	0.001261
15	0.001052	0.001124	0.00118	0.001189	0.001259
17.5	0.001021	0.001075	0.001173	0.001271	0.001271
20	0.001034	0.001144	0.001137	0.001204	0.001243
22.5	0.001047	0.001133	0.00114	0.001191	0.001196
25	0.001032	0.001071	0.001153	0.001225	0.001251
Flat model	0.000979	0.001036	0.001133	0.001195	0.001269

Table 2 The values of differences in pressure drop in channels with different radii of curvature and in the flat channel, %

***R*, mm**	***l*, mm**									
	6	**7**	**8**	**9**	**10**	**11**	**12**	**13**	**14**	**15**
2.5	-5.85	8.25	12.69	6.17	2.76	7.37	4.91	1.37	1.81	2.24
5	0.07	10.50	7.01	6.50	-1.13	5.74	3.18	2.06	5.67	0.53
7.5	-7.26	3.55	8.01	4.74	-3.07	2.73	7.34	2.62	-0.13	3.02
10	-0.87	6.65	3.33	8.80	1.55	6.58	4.21	2.33	1.47	-0.69
12.5	-6.27	6.82	7.36	2.50	4.29	7.95	7.15	1.08	-0.48	-0.68
15	-3.95	5.91	8.41	6.81	-1.93	6.89	7.79	3.95	-0.54	-0.82
17.5	-2.71	4.53	6.94	2.45	0.84	4.07	3.64	3.40	5.95	0.13
20	-6.62	4.01	6.18	1.95	0.79	5.26	9.41	0.30	0.71	-2.11
22.5	9.99	10.10	3.66	3.19	-2.92	6.45	8.53	0.58	-0.33	-6.13
25	-0.31	3.56	5.03	4.94	-1.95	5.09	3.28	1.70	2.41	-1.45

It should be noticed that equation (4) does not include the absolute value sign in the denominator, unlike similar equations in work [41]. This representation allows not only estimating the absolute value of the difference but also observing that the use of the flat model leads to an overestimation of the pressure drop (in this case, the difference will be negative) or such an approach causes an underestimation of this value (the difference will be positive).

In section 2.3, it was pointed out that the attempts to carry out the detailed investigation using the technique applied in work [20] led to controversial results, which was the reason for the change in the geometrical shape of the channels. However, these changes did not allow to eliminate all contradictions in results. The data presented in Tables 1 and 2 show that the pressure drop increased with the increase of the channel length, which also can be seen in Figure 1. However, no monotonic changes in the pressure drop or difference with the flat model are observed when the radius of curvature of the channel changes. Moreover, both underestimation and overestimation of the pressure drop are observed when using the flat model.

At the same time, in the previous work [20], some regularities were observed. In particular, the values of difference of the pressure drops in the flat and ring-shaped channels were slightly decreased with increasing of diameter of the ring-shaped channel.

Therefore, the data obtained in the current work show that the conclusions made in the work [20] appear to be somewhat premature. In particular, the clear dependences of hydrodynamical parameters on the ratio l/d are not observed. Also, the data available at the current stage of investigation do not allow to validate assumption about the existence of some critical value of the channel curvature for values of radius bigger than the critical one the difference with the flat model would be negligible. The determination of the influence of the channel curvature requires a deeper analysis of the factors that impact the transfer processes. This is the objective of further investigation in this direction, including experimental.

It also should be noticed that the appearance of the regularities in the work [20] was most likely a coincidence related to shortcomings in the planning of the CFD study, as outlined in Section 1, particularly the relatively small number of points under investigation.

The available data allows us to make a limited number of assumptions about the reasons of the nonuniformity of the obtained results. One of the probable reasons could be the specific characteristics of CFD methods, which use numerical approaches that have some inherent error. In this case, the magnitude of the difference due to curvature may be of the same order of magnitude as the computational error in the numerical solution. This statement requires further examination, in particular, experimental by the comparison of the obtained differences with the measurement error. This is also the objective of further investigations.

Nevertheless, the obtained values of differences allow us to make some conclusions about the suitability of the application of the flat model.

In work [20], the difference in the pressure drop values in the flat and ring-shaped channels did not exceed 3.2%, and in most cases was less than 1%, which clearly indicated good convergence without the need for further justification. However, in Table 2, differences greater than 10% are observed, with the maximum value reaching 12.69%. Therefore, it is reasonable to consider the conclusions presented in other studies regarding acceptable result accuracy. It should be noticed, that Hostermeier *et al*. [22] made conclusions about significant deviations based on velocity field visualizations in the channel, and Taherinejad *et al*. [25] stated that a difference of more than two times is significant. At the same time, in a significant number of studies, conclusions about agreement were made based on error values expressed as percentages. For example, Qiao *et al*. [42] noted that a good convergence is within 2%. Barbian *et al*. [43] indicated that a pressure drop prediction accuracy of 7.6% is good, Sujanani *et al*. [44] stated that differences under 8% are acceptable, and Giglià *et al*. [45] indicated good agreement with an error of less than 10%. Considering this, an accuracy range of 7-10% can be considered acceptable.

According to Table 2, in the range of curvature radii from 0.01 m (10 mm) to 0.025 m (25 mm) and lengths from 0.008 m (8 mm) to 0.015 m (15 mm), the differences do not exceed 10%, with 14.3% of the investigated points having differences greater than 7%, while in 48% of cases, the differences did not exceed 3.2%, which was the maximum deviation in [20]. Probably, the apparent high accuracy of the results in this study is also a coincidence, particularly due to the relatively small number of study points.

Therefore, in the specified range of sizes of the models under investigation, it seems reasonable to consider the flat model as an acceptable approximation for the membrane module channel element in CFD studies of new spacer designs. However, if the obtained positive effects do not exceed 7-10%, verification with a model that accounts for channel curvature is advisable. In other words, if the investigations on the flat model show that the new spacer design allows for a decrease in the pressure drop or an increase in the mass transfer coefficient of no more than 7%, it is reasonable to carry out the investigation in the curved channels. Also, it should be noted that the main disadvantage of the flat model is that, in most cases, it tends to underestimate the pressure drop compared to models that account for channel curvature.

The differences in the shorted channels are somewhat larger and this fact can be explained by the influence of the hydrodynamic stabilization zone at the entrance to the channel.

3.3 Influence of Mesh Elements Dimensions

In section 2.4, it was pointed out that the value of the mesh element size of $0.1 \cdot 10^{-3}$ m (0.1 mm), used in [20], was not sufficiently substantiated. Therefore, an additional set of simulations was carried out for models with all cross-sections and a length of 0.01 m (10 mm) using different mesh sizes. The mesh element sizes used were $0.1 \cdot 10^{-3}$ m (0.1 mm), $0.075 \cdot 10^{-3}$ m (0.075 mm), $0.05 \cdot 10^{-3}$ m (0.05 mm), and $0.025 \cdot 10^{-3}$ m (0.025 mm). The simulation results are presented in Table 3, which shows the differences in the pressure drop between the flat model and models with different radii of curvature of the channels.

Table 3 The values of the differences in pressure drop in channels with different curvature radii and in the flat channel at different mesh sizes, %

***R*, mm**	**Mesh size δ, mm**			
	0.1	**0.075**	**0.05**	**0.025**
2.5	8.014	1.759	2.762	4.071
5	6.458	3.520	-1.129	-0.275
7.5	4.010	6.866	-3.069	1.703
10	-3.425	2.660	1.553	5.667
12.5	0.031	2.883	4.291	0.666
15	-3.809	2.041	-1.928	2.179
17.5	0.242	2.853	0.842	2.433
20	5.806	2.200	0.789	0.370
22.5	0.675	2.827	-2.916	0.436
25	-1.821	3.074	-1.950	1.459

It can be seen from Table 3 that for mesh sizes of $0.1 \cdot 10^{-3}$ m (0.1 mm) and $0.075 \cdot 10^{-3}$ m (0.075 mm), slightly larger differences and greater inhomogeneity in values are observed. At the same time, for mesh sizes of $0.05 \cdot 10^{-3}$ m (0.05 mm) and $0.025 \cdot 10^{-3}$ m (0.025 mm), differences are significantly smaller. These results suggest that an insufficiently big mesh size can introduce additional errors. However, the excessive decrease in the mesh element size leads to a dramatic increase in the number of mesh elements and, correspondingly, increasing in the required computational power or calculation time. For instance, when the mesh size was reduced from $0.05 \cdot 10^{-3}$ m (0.05 mm) to $0.025 \cdot 10^{-3}$ m (0.025 mm), the calculation time for the models increased by more than 5 times. The obtained results indicate that, for the considered system, the most rational mesh size is $0.05 \cdot 10^{-3}$ m (0.05 mm).

Therefore, the choice of mesh size is a trade-off that balances calculation accuracy with time and computational power requirements. An important parameter is also the minimum geometric size of the object being studied.

3.4 Main Directions of Further Research

In the current work, as well as in the previous study [20], the effect of channel curvature on the pressure drop in the membrane channels was investigated. Although the obtained results do not confirm the assumption that the difference between curved and flat channels decreases with an increasing radius of curvature or the existence of some critical radius of

curvature, taking into account the remarks made in section 3.2, the flat model can be considered as an acceptable approximation of a spiral module channel. However, all these studies were carried out for hypothetical channels without spacers. As was pointed out in [20], the curvature of the spacer can also influence the pressure drop, so this issue is considered the objective of our further research. Additionally, the current work was limited to a single velocity value, and in work [20], only typical values for modules of 1812 type were considered. Bigger values of velocities can lead to different results. It would also be worthwhile to validate the CFD modeling results experimentally.

4.0 CONCLUSION

The CFD investigation of the influence of channel curvature on the pressure drop were carried out. It was defined that in the range of radii of curvature from 0.01 m (10 mm) to 0.025 m (25 mm) and lengths from 0.008 m (8 mm) to 0.015 m (15 mm), the divergence does not exceed 10%. Therefore, the flat model can be considered an acceptable approximation of the real conditions in a spiral module channel, particularly when studying new spacer designs. However, if obtained effects do not exceed 7-10%, the additional investigations considering curvature are advisable.

The assumption of a critical radius of curvature, beyond which the effect of curvature is negligible, was not confirmed.

ACKNOWLEDGEMENT

Authors would like to thank the Armed Forces of Ukraine, National Guard, Territorial Defence, and Volunteers for providing security to perform this work. This work has become possible only because resilience and courage of the Ukrainian Army. We would like also thanks to the international partners of Ukraine which do not leave Ukraine alone at the face of Russian aggression.

The authors would also like to thank Dr. Kateryna Terletska for the valuable advice and recommendations about the selection of simulation conditions.

CONFLICT OF INTEREST

The authors declare no conflicts of interest.

REFERENCES

[1] Hu, X., Li, J., Yu, S., Zhu, Z., Lin, P., & Li, X. (2024). Enhanced mass transfer and energy efficiency by a biomimetic feed spacer in reverse osmosis membrane modules. *Journal of Membrane Science*, 123290. https://doi.org/10.1016/j.memsci.2024.123290.

[2] Yang, S., Shang, W., Yang, R., Shi, H., Zeng, H., Xing, D., Sun, F., & Xiong, X. (2024). Synergistically controlling biofouling and improving membrane module permeability by using simultaneously structurally optimized and surface modified feed spacers. *Journal of Membrane Science, 708*, 123046. https://doi.org/10.1016/j.memsci.2024.123046.

[3] Jeong, Y., Jeong, S., Jeong, S., & Gu, B. (2024). Helical strip-type spacers for enhanced multi-directional mixing and mitigation of temperature polarisation in

membrane distillation – A numerical and experimental investigation. *Journal of Membrane Science*, *707,* 122987. https://doi.org/10.1016/j.memsci.2024.122987.

[4] Huliienko, S. V., Korniyenko, Y. M., Muzyka, S. M., & Holubka, K. (2022). Simulation of reverse osmosis process: novel approaches and development trends. *Journal of Engineering Sciences*, *9*(2), F6–F36. https://doi.org/10.21272/jes.2022.9(2).f2.

[5] Johnston, J., Dischinger, S. M., Nassr, M., Lee, J. Y., Bigdelou, P., Freeman, B. D., Gleason, K. L., Martinand, D., Miller, D. J., Molins, S., Spycher, N., Stringfellow, W. T., & Tilton, N. (2023). A reduced-order model of concentration polarization in reverse osmosis systems with feed spacers. *Journal of Membrane Science*, *675*, 121508. https://doi.org/10.1016/j.memsci.2023.121508.

[6] Bae, S., Gu, B., & Lee, J. H. (2023). A 3D CFD study on the effects of feed spacer designs on membrane performance for high-permeance RO membranes. *Journal of Water Process Engineering*, *53*, 103887. https://doi.org/10.1016/j.jwpe.2023.103887.

[7] Yang, S., Shang, W., Shi, H., Sun, F., & Zeng, H. (2023). Development of an automatic and object-oriented method for spacer design in the spiral wound nanofiltration modules to comprehensively enhance filtration performance. *Desalination*, *566*, 116945. https://doi.org/10.1016/j.desal.2023.116945.

[8] Park, S., Jeong, Y. D., Lee, J. H., Kim, J., Jeong, K., & Cho, K. H. (2020). 3D printed honeycomb-shaped feed channel spacer for membrane fouling mitigation in nanofiltration. *Journal of Membrane Science*, *620*, 118665. https://doi.org/10.1016/j.memsci.2020.118665.

[9] Sreedhar, N., Mavukkandy, M. O., Aminabhavi, T. M., Hong, S., & Arafat, H. A. (2022). Fouling mechanisms in ultrafiltration under constant flux: Effect of feed spacer design. *Chemical Engineering Journal*, *446*, 136563. https://doi.org/10.1016/j.cej.2022.136563.

[10] Baitalow, K., Wypysek, D., Leuthold, M., Weisshaar, S., Lölsberg, J., & Wessling, M. (2021). A mini-module with built-in spacers for high-throughput ultrafiltration. *Journal of Membrane Science*, *637*, 119602. https://doi.org/10.1016/j.memsci.2021.119602.

[11] Zhang, Z., Zhang, N., Xiang, B., Yuan, Y., & Phelan, P. E. (2023). Numerical investigation on mass and heat transfer performance for novel vacuum membrane distillation modules enhanced by semicircular spacers. *International Journal of Thermal Sciences*, *187*, 108165. https://doi.org/10.1016/j.ijthermalsci.2023.108165.

[12] Ansari, A., Galogahi, F. M., Millar, G., Helfer, F., Thiel, D. V., Soukane, S., & Ghaffour, N. (2022). Computational fluid dynamics simulations of solar-assisted, spacer-filled direct contact membrane distillation: Seeking performance improvement. *Desalination*, *545*, 116181. https://doi.org/10.1016/j.desal.2022.116181.

[13] Stockmeier, F., Stüwe, L., Kneppeck, C., Musholt, S., Albert, K., Linkhorst, J., & Wessling, M. (2023). On the interaction of electroconvection at a membrane interface with the bulk flow in a spacer-filled feed channel. *Journal of Membrane Science*, *678*, 121589. https://doi.org/10.1016/j.memsci.2023.121589.

[14] Al-Amshawee, S. K. A., & Yunus, M. Y. B. M. (2023). Impact of membrane spacers on concentration polarization, flow profile, and fouling at ion exchange membranes of electrodialysis desalination: Diagonal net spacer vs. ladder-type configuration. *Process Safety and Environmental Protection*, *191*, 197–213. https://doi.org/10.1016/j.cherd.2023.01.012.

[15] Ali, S. M., Kim, Y., Qamar, A., Naidu, G., Phuntsho, S., Ghaffour, N., Vrouwenvelder, J. S., & Shon, H. K. (2021). Dynamic feed spacer for fouling minimization in forward osmosis process. *Desalination*, *515*, 115198. https://doi.org/10.1016/j.desal.2021.115198.

[16] Goi, Y., Liang, Y., Lau, W., & Weihs, G. F. (2022). Analysis of the effect of advanced FO spacer on the specific energy consumption of hybrid RO desalination system. *Journal of Membrane Science*, *668*, 121247. https://doi.org/10.1016/j.memsci.2022.121247.

[17] Cai, J. J., Hawboldt, K., & Abdi, M. A. (2016). Analysis of the effect of module design on gas absorption in cross flow hollow membrane contactors via computational fluid dynamics (CFD) analysis. *Journal of Membrane Science*, *520*, 415–424. https://doi.org/10.1016/j.memsci.2016.07.054.

[18] Cancilla, N., Gurreri, L., Marotta, G., Ciofalo, M., Cipollina, A., Tamburini, A., & Micale, G. (2022). A porous media CFD model for the simulation of hemodialysis in hollow fiber membrane modules. *Journal of Membrane Science*, *646*, 120219. https://doi.org/10.1016/j.memsci.2021.120219.

[19] Mohan, T. R., Kumar, M., & Rao, L. (2022). Biofouling of hollow fiber ultrafiltration membranes: A novel multiphase CFD – Porous - CES model and experimental study. *Journal of Membrane Science*, *663*, 121034. https://doi.org/10.1016/j.memsci.2022.121034.

[20] Huliienko, S., Korniyenko, Y., & Yasenchuk, V. (2024). Evaluation of the influence of the channel curvature on the flow characteristics in the channel of spiral wound membrane modules using CFDOF. In *Lecture Notes on Data Engineering and Communications Technologies* (pp. 441–453). https://doi.org/10.1007/978-3-031-71801-4_32.

[21] Haaksman, V. A., Siddiqui, A., Schellenberg, C., Kidwell, J., Vrouwenvelder, J. S., & Picioreanu, C. (2016). Characterization of feed channel spacer performance using geometries obtained by X-ray computed tomography. *Journal of Membrane Science*, *522*, 124–139. https://doi.org/10.1016/j.memsci.2016.09.005.

[22] Horstmeyer, N., Lippert, T., Schön, D., Schlederer, F.,

Picioreanu, C., Achterhold, K., Pfeiffer, F., & Drewes, J. E. (2018). CT scanning of membrane feed spacers – Impact of spacer model accuracy on hydrodynamic and solute transport modeling in membrane feed channels. *Journal of Membrane Science*, *564*, 133–145. https://doi.org/10.1016/j.memsci.2018.07.006.

[23] Lau, K., Bakar, M. A., Ahmad, A., & Murugesan, T. (2009). Feed spacer mesh angle: 3D modeling, simulation and optimization based on unsteady hydrodynamic in spiral wound membrane channel. *Journal of Membrane Science*, *343*(1–2), 16–33. https://doi.org/10.1016/j.memsci.2009.07.001.

[24] Johannink, M., Masilamani, K., Mhamdi, A., Roller, S., & Marquardt, W. (2015). Predictive pressure drop models for membrane channels with non-woven and woven spacers. *Desalination*, *376*, 41–54. https://doi.org/10.1016/j.desal.2015.07.024.

[25] Taherinejad, M., Moghimi, M., & Derakhshan, S. (2019). Hydrodynamic modeling of the spiral-wound membrane module including the membrane curvature: reverse osmosis case study. *Korean Journal of Chemical Engineering*, *36*(12), 2074–2084. https://doi.org/10.1007/s11814-019-0372-1.

[26] Saliakellis, P., Koutsou, C., & Karabelas, A. (2022). The effect of gap reduction on fluid dynamics and mass transfer in membrane narrow channels filled with novel spacers—A detailed computational study. *Membranes*, *13*(1), 20. https://doi.org/10.3390/membranes13010020.

[27] Huliienko, S., & Leshchenko, O. (2019). Influence of operating pressure on concentration polarization layer resistance in revers osmosis. *Ukrainian Food Journal*, *8*(1), 119–132. https://doi.org/10.24263/2304-974x-2019-8-1-13.

[28] Kaufman, Y., Kasher, R., Lammertink, R. G., & Freger, V. (2012). Microfluidic NF/RO separation: Cell design, performance and application. *Journal of Membrane Science*, *396*, 67–73. https://doi.org/10.1016/j.memsci.2011.12.052.

[29] Al-Sharif, S., Albeirutty, M., Cipollina, A., & Micale, G. (2013). Modelling flow and heat transfer in spacer-filled membrane distillation channels using open source CFD code. *Desalination*, *311*, 103–112. https://doi.org/10.1016/j.desal.2012.11.005.

[30] Wang, Y., He, W., & Zhu, H. (2016). Computational fluid dynamics (CFD) based modelling of osmotic energy generation using pressure retarded osmosis (PRO). *Desalination*, *389*, 98–107. https://doi.org/10.1016/j.desal.2016.02.002.

[31] Kang, P. K., Lee, W., Lee, S., & Kim, A. S. (2017). Origin of structural parameter inconsistency in forward osmosis models: A pore-scale CFD study. *Desalination*, *421*, 47–60. https://doi.org/10.1016/j.desal.2017.05.018.

[32] Harandi, H. B., Asadi, A., Fathi, H., & Sui, P. (2021). Combined macroscopic and pore scale modeling of direct contact

membrane distillation with micro-porous hydrophobic membranes. *Desalination*, *514*, 115171. https://doi.org/10.1016/j.desal.2021.115171.

[33] Gruber, M., Johnson, C., Tang, C., Jensen, M., Yde, L., & Hélix-Nielsen, C. (2011). Computational fluid dynamics simulations of flow and concentration polarization in forward osmosis membrane systems. *Journal of Membrane Science*, *379*(1–2), 488–495. https://doi.org/10.1016/j.memsci.2011.06.022.

[34] Haddadi, B., Jordan, C., Miltner, M., & Harasek, M. (2018). Membrane modeling using CFD: Combined evaluation of mass transfer and geometrical influences in 1D and 3D. *Journal of Membrane Science*, *563*, 199–209. https://doi.org/10.1016/j.memsci.2018.05.040.

[35] Liu, X., Xiao, C., Deng, H., Zhang, T., & Huang, Y. (2023). An experimental and modeling investigation of the behaviors of solution in fluoropolymers hollow fiber membranes (HFMs). *Journal of Membrane Science*, *671*, 121421. https://doi.org/10.1016/j.memsci.2023.121421.

[36] Geraldes, V., Henriques, P., Afonso, M. D., Alves, A. M., Pires, R. F., Faria, M., Van Der Bruggen, B., & Rodrigues, M. (2024). Designing centrifugal membrane filters with uniform-pressure for UF/NF/RO separations. *Journal of Membrane Science*, *702*, 122752. https://doi.org/10.1016/j.memsci.2024.122752.

[37] Raach, H., Somasundaram, S., & Mitrovic, J. (2010). Optimisation of turbulence wire spacing in falling films performed with OpenFOAM. *Desalination*, *267*(1), 118–119. https://doi.org/10.1016/j.desal.2010.09.012.

[38] Panda, S. K., Singh, K., Shenoy, K., & Buwa, V. V. (2016). Numerical simulations of liquid-liquid flow in a continuous gravity settler using OpenFOAM and experimental verification. *Chemical Engineering Journal*, *310*, 120–133. https://doi.org/10.1016/j.cej.2016.10.102.

[39] Bhusare, V., Dhiman, M., Kalaga, D., Roy, S., & Joshi, J. (2017). CFD simulations of a bubble column with and without internals by using OpenFOAM. *Chemical Engineering Journal*, *317*, 157–174. https://doi.org/10.1016/j.cej.2017.01.128.

[40] Marcato, A., Boccardo, G., & Marchisio, D. (2021). A computational workflow to study particle transport and filtration in porous media: Coupling CFD and deep learning. *Chemical Engineering Journal*, *417*, 128936. https://doi.org/10.1016/j.cej.2021.128936.

[41] Liang, Y., Dudchenko, A. V., & Mauter, M. S. (2022). Inadequacy of current approaches for characterizing membrane transport properties at high salinities. *Journal of Membrane Science*, *668*, 121246. https://doi.org/10.1016/j.memsci.2022.121246.

[42] Qiao, Z., Guo, Y., Wang, Z., & Hu, G. (2022). A chemically enhanced backwash model for predicting the instantaneous transmembrane pressure of flat sheet membranes in constant

flow rate mode. *Journal of Membrane Science*, *666*, 121137. https://doi.org/10.1016/j.memsci.2022.121137.

[43] Barbian, K. P., Hirschwald, L. T., Linkhorst, J., Neidlin, M., Steinseifer, U., Wessling, M., Wiegmann, B., & Jansen, S. V. (2023). Flow and mass transfer prediction in anisotropic TPMS-structures as extracorporeal oxygenator membranes using reduced order modeling. *Journal of Membrane Science*, *690*, 122160. https://doi.org/10.1016/j.memsci.2023.122160.

[44] Sujanani, R., Reimund, K. K., Gleason, K. L., & Freeman, B. D. (2024). Hydraulic permeation-induced water concentration gradients in ion exchange membranes. *Journal of Membrane Science*, *705*, 122858. https://doi.org/10.1016/j.memsci.2024.122858.

[45] Giglia, S., Rautio, K., Kazan, G., Backes, K., Blanchard, M., & Caulmare, J. (2010). Improving the accuracy of scaling from discs to cartridges for dead end microfiltration of biological fluids. *Journal of Membrane Science*, *365*(1–2), 347–355. https://doi.org/10.1016/j.memsci.2010.09.032.